A Simulation Study of Proportional Resonant Controller Based on the Implementation of Frequency-Adaptive Virtual Flux Estimation with the LCL Filter

Nurul Fazlin Roslan[1], Jon Are Suul[2,3], Alvaro Luna[1], Ignacio Candela[1], Pedro Rodriguez[1,4]
[1] Technical University of Catalonia,
Research Center on Renewable Electrical Energy Systems (SEER Center),Terrassa, Spain
[2] Norwegian University of Science and Technology, Trondheim, Norway
[3]SINTEF Energy Research, Trondheim, Norway
[4]Abengoa Research, Sevilla, Spain
nurulfazlin@unikl.edu.my,jon.are.suul@ntnu.no,luna@ee.upc.edu, candela@ee.upc.edu, prodriguez@ee.upc.edu,

***Abstract*—This paper discusses the implementation of proportional resonant (PR) current controllers for a Voltage Source Converter (VSC) with LCL filter which is synchronized to the grid by virtual flux (VF) estimation with inherent sequence separation. Even though there is an extensive amount of literature and studies on the PR current controller for tracking the current reference of a VSC in the stationary reference frame, there is no discussion taking into account voltage sensor-less operation based on virtual flux estimation with an LCL-filter. Separate estimation of the positive and negative sequence virtual flux components at the grid-side of the LCL-filter, as well as current sequence separation, using the Second Order Generalized Integrator-Frequency Locked Loop (SOGI-FLL) is presented as part of a proposed method. The LCL filter is characterized in order to reduce the parameter deviation that might affect the virtual flux estimation. The stability of the proposed method is analyzed in the frequency domain while the operation and performance of the proposed system is verified by simulation studies.**

Keywords—Virtual Flux Estimation, Sensor-less Control, Grid Synchronization, Proportional Resonant, Current Controller, Voltage Source Converter, Stability Limit.

I. INTRODUCTION

Rapid changes in the world energy supply is posing new demands and challenges on the ac network and the control of power electronic converters for grid conection of generation sources and loads [1]. As the application of grid connected or stand-alone Voltage Source Converters (VSCs) has evolved, voltage sensor-less operation has become an attractive solution because it can reduce costs by means of reducing the number of sensors needed, which also contributes to increase the system modularity [2]. Estimation methods based on the Virtual Flux (VF) concept is one of the approaches that can be implemented to achieve voltage sensor-less grid synchronization [3]. With known parameter values of the grid-side filter, duty cycle as well as the converter output current, which is normally measured, the VF estimation is capable of estimating the grid voltage conditions and ensuring reliable grid synchronization without ac voltage measurements. In conventional system, the point of synchronization is fixed at the location of the voltage measurements, while an advantage of VF estimation it that, it is possible to perform an estimation at remote points in the grid [4], [5]. This is offerring a flexible way to control the active and reactive power flows [6]. However, the complexity of the implementation depends on the estimation method and the filter configuration.

An early comparative study of voltage sensor-less control for the PWM rectifier based on direct power control and on voltage oriented control was presented by Hansen et al in [2]. Subsequently, Malinowski et al. proposed the voltage sensorless operation based on VF estimation using direct power control [3]. The work in [3] was improved in [7] with the used of space vector modulation and a slow PLL applied in order to track the positive sequence of the estimated VF. A further comparative study was presented in [8] where the method in [2] was compared with the performance of [3] and [7]. Another study was later conducted by Jasinki et al. in [9], where notch filters and low pass filters were aplied in the Positive Sequence Synchronous Reference Frame (PS-SRF) in order to cancel out the influence of negative sequence grid voltage components on the VF estimation.

In [10], the first study of VF based voltage sensor-less controlled taking into consideration the estimation of both positive and negative sequence virtual flux (PNS-VF) components in the stationary reference frame was presented by Kulka. The VF estimation was implemented by cascading two low pass filters with cut off frequency identical to the grid frequency, produce a 90° phase shift for the VF estimation. In practical implementation, a drift compensation solution was included to achieve offset free VF to overcome the sensitivity of the system in case of grid frequency

variations [10]. The development of an online frequency-adaptive VF based approach for voltage sensor-less control of the grid integrated VSC under unbalanced condition was later studied in details in [11], [12], [13]. VF-based power control under unbalanced conditions, including strategies for operating under current limitation was also analyzed in [11]. The voltage sensor-less grid synchronization was achieved by means of the frequency adaptive VF estimation, taking advantage of the Second Order Generalized Integrator Configured as a Quadrature SignalGenerator (SOGI-QSG). The frequency adaptive dual SOGI-based VF estimation (DSOGI-VF) with inherent sequence separation was first proposed in [12] with the objective to simplify the method used in [10] and to avoid cascaded flux estimation and sequence separation that could lead to relatively slow transients. However sequence separation of current is needed in the work done in [11], [12], [13], [5] since the current induced flux needs to be subtracted separately for each sequence component once the positive and negative sequence VF have been estimated.

It should be noted that all the mentioned studies of the VF estimation approach are based on the analysis of grid connected VSC with the L-filter and LC-filter. Beyond a recent example in [14], the case of VF estimation with LCL-filters has to the best knowledge of the authors, not been given great attention by researchers in the past and this motivated the present study. In [14], only a PS-SRF current controller was applied, while in this paper the VF based estimation with the LCL filter is proposed together with Proportional Resonant (PR) current controller used as the inner part of the control system. The PR current controller is used to control the converter output current by forcing it to follow the reference current. The VF estimation in this paper is expected to have no error on the phase displacement and amplitude so that the system can perform an ideal tracking without any delay and provide a good dynamic response since the cascaded structure of sequence separation is avoided. The work starts with an overview of voltage sensor-less grid synchronization based on VF estimation where the proposed method will be highlighted. This is continued by a discussion of LCL filters and the PR current controllers used in this work. Further on, the stability analysis and the simulation results are discussed before concluding the paper with a discussion of performance obtained with the PR controller based on the VF estimation with the LCL filter.

II. Voltage Sensor-Less Grid Synchronization Based on Virtual Flux Estimation

A. Virtual Flux Definition

The virtual flux (VF), Ψ can be defined from the integral of the converter output voltage V and it can be estimated based on the DC-link voltage and the reference signal for the Pulse Width Modulation (PWM) of the converter. Considering the flux calculation in the stationary reference frame, the VF can be considered in (1) as explained in [3], [10], [12][11].

$$\Psi_{\alpha\beta} = \int V dt + \Psi_0 \tag{1}$$

B. Proposed Method for Frequency-Adaptive Dual SOGI based Virtual Flux estimation (DSOGI-VF) with Sequence Separation of Fluxes and Currents

The proposed control structure used in this paper is shown in Fig. 1. The applied VF-based synchronization method is similar to [11], [12], [13], and is based on the DSOGI-FLL. The structure of DSOGI-VF consists of the dual SOGI-QSG, frequency locked loop (FLL) and positive-negative sequence calculation (PNSC) network, based on the implementations explained in [1]. The basic structure of SOGI-QSG is shown in Fig. 2 where the v' is the direct output from input signal v whereas the qv' represents the in-quadrature output signal from v' which is an integral of output v' multiplied with the frequency ω'[1]. If v is a sinusoidal signal, v' and qv' will always be sinusoidal but the in-quadrature output qv' will be 90° lagging v', independently of both frequency of v and the values of ω' and k.

The value of $k = \sqrt{2}$ will results in a good compromise between overshoot and stabilization time [12], [1] and hence will be used in this study. The 90° phase shifted for sequence separation is available from the output of v'. Considering that the output is the derivative of VF, changing the sign will corresponds to 90° phase lag as shown in Fig. 3. The transfer function of the output v' with respect to the input v and the in-quadrature output qv' with respect to v' is given by (2) and (3) respectively.

$$\frac{v'}{v}(s) = \frac{k\omega' s}{s^2 + k\omega' s + \omega'^2} \tag{2}$$

$$\frac{qv'}{v}(s) = \frac{k\omega'^2}{s^2 + k\omega' s + \omega'^2} \tag{3}$$

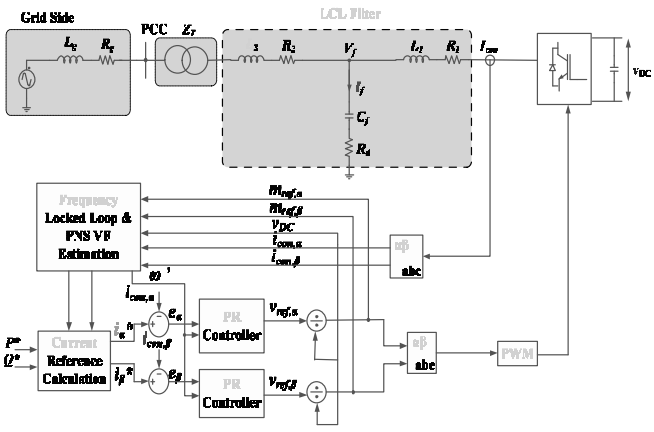

Fig. 1. The proposed structure of PR current controller based on Frequency Adaptive DSOGI-VF Estimation with LCL Filter

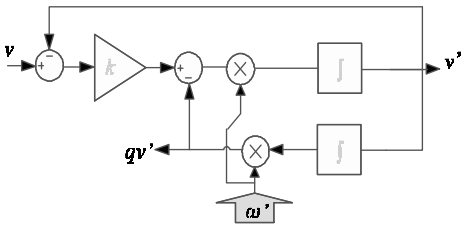

Fig. 2. Basic structure of SOGI-QSG block.

The VF estimation is based on the current measurement at the converter side, I_{con} and the method of estimation is shown in Fig. 3. The resistive voltage drop at the R_1 is subtracted from the converter output voltage and the inductive flux drop of L_1 is subtracted from the integrated voltage in the same way as [11]. The converter output current is transformed into alpha-beta component and is referred to as $i_{con,\alpha\beta}$ throughout this analysis. Since the LCL filter has been considered in the proposed method, the capacitor current need to be taken into account by estimating the capacitor current, i_f from the estimated capacitor voltage, V_f.

To avoid measuring another current, the grid current, $i_{g,\alpha\beta}$ is estimated by subtracting the capacitor current i_f from the inverter current $i_{con,\alpha\beta}$. Thus the integral of grid current is needed [11]. The resulting estimation of the VF at the grid side of the filter inductor is given by (4) with neglecting the resistance in the transformer. The impact of the resistive voltage drop at the grid side is determined by multiplying the R_2 with the integral of grid current. The inductive flux drop at the grid side is considered by multiplying the grid current with added value of L_2 and L_T where the L_T is derived from the transformer impedance which is 5% of the base impedance value.

For scaling purposes, the VF estimation in (4) can be transformed into per unit values by dividing the base value of the flux as given in (5) where the V_b is the peak value of the rated phase voltage and ω_b is the nominal angular frequency. The per unit VF model without considering the correction term is given by (6). According to [11] and [12], the suggested base value for the DC-link voltage is two times the value of V_b.

$$\Psi_{\alpha\beta} = \int\left(m_{ref\alpha\beta}\cdot\frac{1}{2}V_{DC} - (R_1\cdot I_{con,\alpha\beta})\right)dt - (L_1\cdot I_{con,\alpha\beta}) - (R_2\cdot \vartheta I_{g,\alpha\beta}) - \left[(I_{con,\alpha\beta} - I_{f,\alpha\beta})\cdot(L_2+L_T)\right] \tag{4}$$

$$\Psi_b = \frac{V_b}{\omega_b} \tag{5}$$

$$\Psi_{\alpha\beta} = \int\left(m_{ref\alpha\beta}\cdot v_{DC} - (r_1\cdot i_{con,\alpha\beta})\right)dt - (l_1\cdot i_{con,\alpha\beta}) - (r_2\cdot \vartheta i_{g,\alpha\beta}) - \left[(i_{con,\alpha\beta} - i_{f,\alpha\beta})\cdot(l_2+l_t)\right] \tag{6}$$

The resulting VF after considering the per unit values can be expressed by the letter χ where the flux model is multiplied with the per unit frequency of the system as given by (7) and (8) respectively.

$$\chi(t) = \omega_{pu}\cdot\omega_b\int v dt \tag{7}$$

$$\chi^{\alpha\beta}(t) = \omega_{pu}\cdot\omega_b\int(v_{ref\alpha\beta}\cdot v_{DC} - (r_1\cdot i_{con,\alpha\beta}))dt - (l_1\cdot i_{con,\alpha\beta}(t)) - (\vartheta i_{g,\alpha\beta}(t)\cdot r_2) - [(l_2+l_t)\cdot(i_{con,\alpha\beta}(t) - i_{f,\alpha\beta}(t))] \tag{8}$$

Applying (3) into (8) where the output $qv' = \chi$, leads to the transfer function in (9).

$$\chi^{\alpha\beta}(s) = \left[\frac{k\omega'^2}{s^2+k\omega' s+\omega'^2}\cdot v_{\alpha\beta}(s) - [(r_1\cdot i_{con,\alpha\beta}(s)]\right] - [\omega_{pu}\cdot(l_1\cdot i_{con,\alpha\beta}(s))] - \left[\frac{k\omega'^2}{s^2+k\omega' s+\omega'^2}\cdot i_{g,\alpha\beta}(s)\cdot r_2\right] - [\omega_{pu}\cdot([l_2+l_t]\cdot[i_{con,\alpha\beta}(s) - i_{f,\alpha\beta}(s)])] \tag{9}$$

The output of the virtual flux estimation shown in Fig. 3 will later be used in determining the current reference i_α^* and i_β^* and it will be injected into the current controller as shown in Fig. 1. The current reference i_α^* and i_β^* have been obtained based on the active and reactive power equation. The currents and voltages, however, have been transformed into the α-β reference frame according to the Clark Transformation [1]. By taking into account the VF estimation carried out in Fig. 3, the current reference i_α^* and i_β^* can be established by (10) and (11) accordingly when sinusoidal balanced currents should be obtained independently of any unbalance in the grid voltage [11], [1]. These equations have been formulated in PSIM to generate the current references needed for the SOGI-based PR controller. Since the PR controlleris also based on the SOGI structure, the frequency needed by this component is supplied by the frequency locked loop (FLL).

$$i_\alpha^* = \left[\frac{P_{ref}\cdot\chi^+_{g,\alpha} + Q_{ref}\cdot\chi^+_{g,\beta}}{{\chi^+_{g,\alpha}}^2 + {\chi^+_{g,\beta}}^2}\right] + i_{f,\alpha} \tag{10}$$

$$i_\beta^* = \left[\frac{P_{ref}\cdot\chi^+_{g,\beta} - Q_{ref}\cdot\chi^+_{g,\alpha}}{{\chi^+_{g,\alpha}}^2 + {\chi^+_{g,\beta}}^2}\right] + i_{f,\beta} \tag{11}$$

In balanced condition, the α-component as well as the β-component is expected to have equal amplitude. The β component, however, will be lagging the α-component by 90° in time and phase displacement [11], [12].

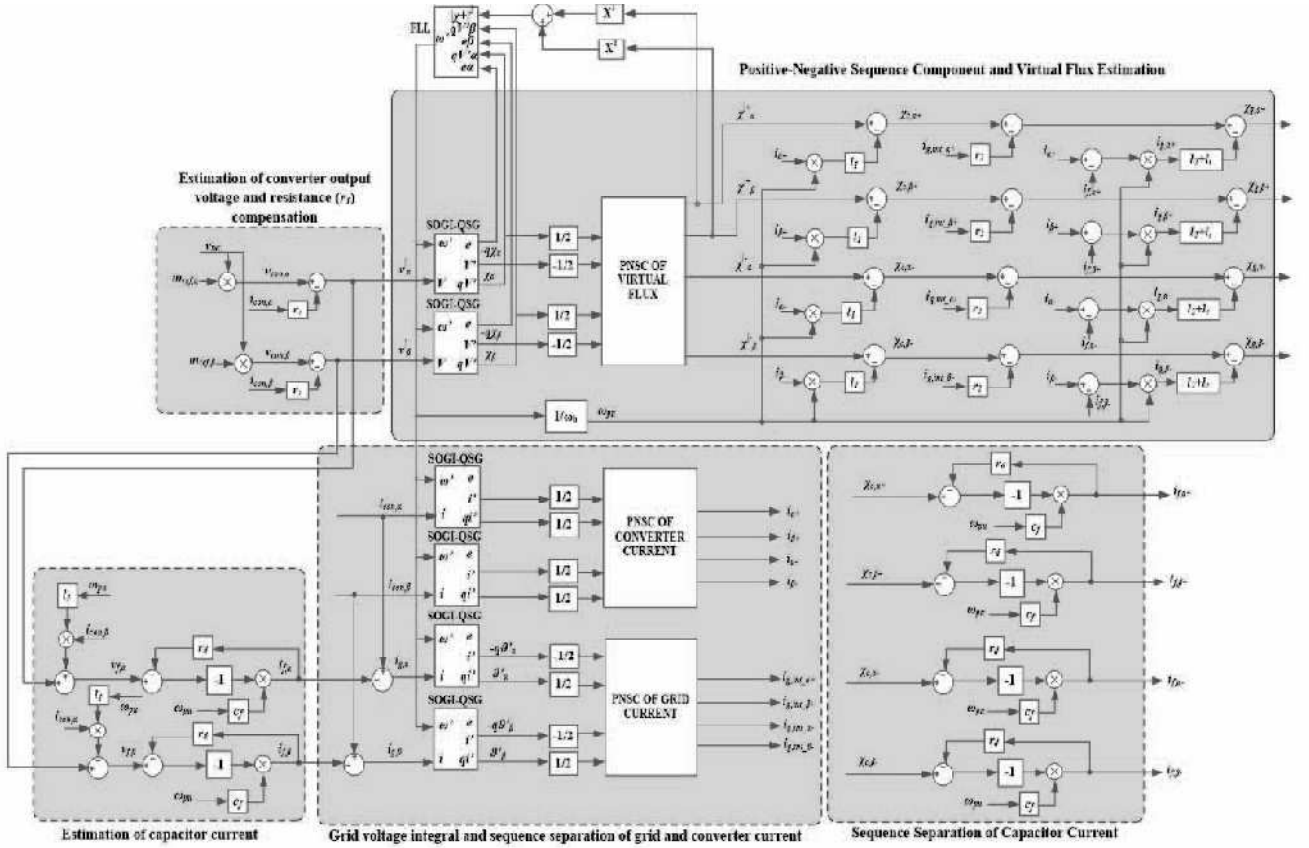

Fig. 3. Proposed Structure of Frequency Adaptive of Dual SOGI based on Virtual Flux (DSOGI-VF) including the Positive-Negative Sequence Components (PNSC) with the LCL Filter considering the current sensor sensed the current at the converter side of the filter

III. LCL FILTER AND CURRENT CONTROLLER

A. Characterization of LCL Filter

A very simple approach done by Liserre and Reznik in [15] and [16] has been used to properly calculate and obtain the values of the LCL filters used in this paper. The10kW system has been considered and the system parameters of the LCL filter that have been obtained by using the design procedure listed in [16] are shown in Table I. In this paper, the passive damping resistor in series with the capacitor has been included in the design of the filter and leads to the transfer function in (12).

TABLE I. SYSTEM PARAMETERS

Parameters		
Abbreviation	***Nomenclature***	***Values***
P_n	Nominal Rated Power	10kW
V_g	Phase Grid Voltage	230V
V_{DC}	DC link Voltage	685V
f_{sw}	Switching Frequency	10kHz
f_g	Grid Frequency	50Hz
L_1	Inverter Side Inductor	0.00557H
L_2	Grid Side Inductor	0.00151H
L_T	Transformer Inductor	0.00254H
C_f	Capacitor Filter	39.8µF
R_d	Damping Resistor	1.81995Ω

$$G_{F,d}(s) = \frac{C_f R_d s + 1}{L_1 C_f L_2 s^3 + C_f (L_1 + L_2) R_d s^2 + (L_1 + L_2) s} \tag{12}$$

B. Proportional Resonant Current Controller

The principle of the Proportional Resonant Controller (PR) is based on the second order generalized integrator (GI) concept [1]. Equation (13) presents an ideal PR controller which can give stability problems according to [17] because of an infinite gain. To avoid this condition, the PR controller can be treated as non-ideal by introducing damping as stated in (14). The K_p is the proportional gain which is possible to control the dynamics of the system and K_r is the integral gain term. By using the PR controller, the tracking capability of the current reference can be ensured and the simplicity in the implementation of the current controller is enhanced compared to the conventional synchronous Proportional Integral (PI) controller. This is one of the reasons for the extensive use of PR controllers.

$$G_{PR}(s) = K_p + K_r \frac{s}{s^2 + \omega_o^2} \tag{13}$$

$$G_{PR}(s) = K_p + K_r \frac{2\omega_c s}{s^2 + 2\omega_c s + \omega_o^2} \tag{14}$$

The transfer function in (13) will give a very small and almost null bandwidth if compared to the non-ideal cases in (14) where the ω_c can be widened or narrowed to control the bandwidth [17]. The smaller value of ω_c, the more sensitive the filter to the frequency variations and it will also leads to a slower transient response. A value of ω_c in the range of 5-15rad/s will provide a good compromise in practice [18]. The system bandwidth can also be controlled by setting the value of K_r. Relatively, the higher the values of K_r is used, the larger the bandwidth could be and vice versa. If the value of K_p is increased, it will increase the magnitude and by increasing the values of the ω_c both magnitude and phase will be increased.

IV. Stability Analysis and Simulation Result of the Proposed Method

A. Stability Analysis

The system stability is very important to ensure that the current controller is working on the optimal performance within its stability region. Theoretically the higher the values of the Proportional Gain, K_r, the higher ability of the PR controller to track the current reference, leading to a high tracking capability compared to low values of K_r. However the stability limit must be taken into account to satisfy the statement. The whole system is defined as a stable system if the closed loop system is also in a stable condition. A stable system is expected to have a frequency response at the closed loop system that decays over time. The closed loop system will be unstable if the frequency response is larger over time. The closed loop system of current controller including the PR current controller, processing delay and filter in continuous domain is shown in Fig. 4 where the I_{in} is the inverter output current which is used as a feedback, U_{in}^* is the inverter voltage reference and the I_{in}^* is the inverter current reference [17].

The continuous domain equation for the PR controller and the filter is based on (14) and (12) respectively. The processing delay equation is given by (15) where the T_s is the sample time [17]. The transfer function of the closed loop system can be derived by (16) where the 'c2d' function in MATLAB has been used to convert from continuous domain to the discrete domain by means of the zero order hold (ZOH) method. In practice, there are a lot of methods other than ZOH for discretization such as First Order Hold, Forward Euler, Backward Euler, Tustin, Tustin with Prewarping, Zero-pole Matching and Impulse Invariant. However, the ZOH provides a good representation of the average voltage output from the converter PWM operation on the filter inductor during one sampling period.

$$G_D(s) = \frac{1}{1 + sT_s} \tag{15}$$

$$C_L(z) = \frac{G_{PR}(z) \cdot G_D(z) \cdot G_{F,d}(z)}{1 + G_{PR}(z) \cdot G_D(z) \cdot G_{F,d}(z)} \tag{16}$$

The other elements that are very important in stability analysis are the gain and phase margin. If the system has lower margin it means that it is less stable. The best way to describe the margin is how far it is from the unstable point where for the gain margin the unstable point is at 0dB gain while the unstable point for the phase margin is at -180° phase. The system will be stable if both the gain and phase margin in the open loop system is positive. Initially the K_p used in the simulation is 9.789 which the value is calculated based on PI current controller concept. Even though the system is stable, the gain and phase margin is relatively low as compared to a good and stable system, which should at least have a phase margin of 60°.

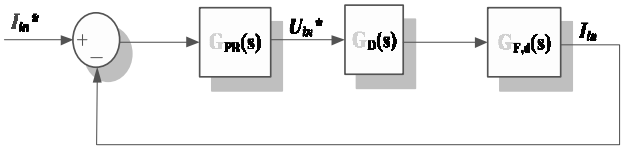

Fig. 4. The PR current controller structure.

The stability of the system has been studied by using the SISO tool in MATLAB. The simulation has been done with K_p values ranging from 5 to 9 while the K_r values are kept constant at 6000 where the ω_c and ω_o is equal to 314 rad/s. The stability status has been summarized in Table II. Based on the results obtained in Table II, to get a stable system with the phase margin of at least 60° - 70° and the gain margin ≥ 3dB, the K_p value can't be lower than 5.5 and higher than 8 with the K_r is kept constant at 6000. To get at least 60° phase margin, the K_p should be tuned to 5.6 where the gain margin of the open loop system is at 5.24dB.

TABLE II. System Stability

K_p Value	Stability Status		
	Closed Loop and Open Loop Status	*Gain Margin (dB)*	*Phase Margin (°)*
5	Stable	5.69	57.6
5.5	Stable	5.32	59.7
5.6	Stable	5.24	60.1
5.8	Stable	5.10	60.9
6	Stable	4.96	61.8
7	Stable	4.27	65.8
8	Stable	3.64	69.0
9	Stable	3.05	23.2

The root locus and bode diagram of the open loop system is shown in Fig. 5(a) and the bode diagram of the closed loop system and step response is shown in Fig. 5(b) respectively. If the K_p is tuned to 5.6, the limit of the K_r value would be below than 16000. It can be observed from Fig. 6(a) that the system is still stable when the K_r = 15000 and the loop is unstable when K_r = 16000 where both the gain and phase margin become negative as shown in Fig. 6(b). Even though the system is stable when K_r = 15000, the values of the gain and phase margin are too low and system can experience instability during transient responses. Hence tuning in this range is not recommended to be used.

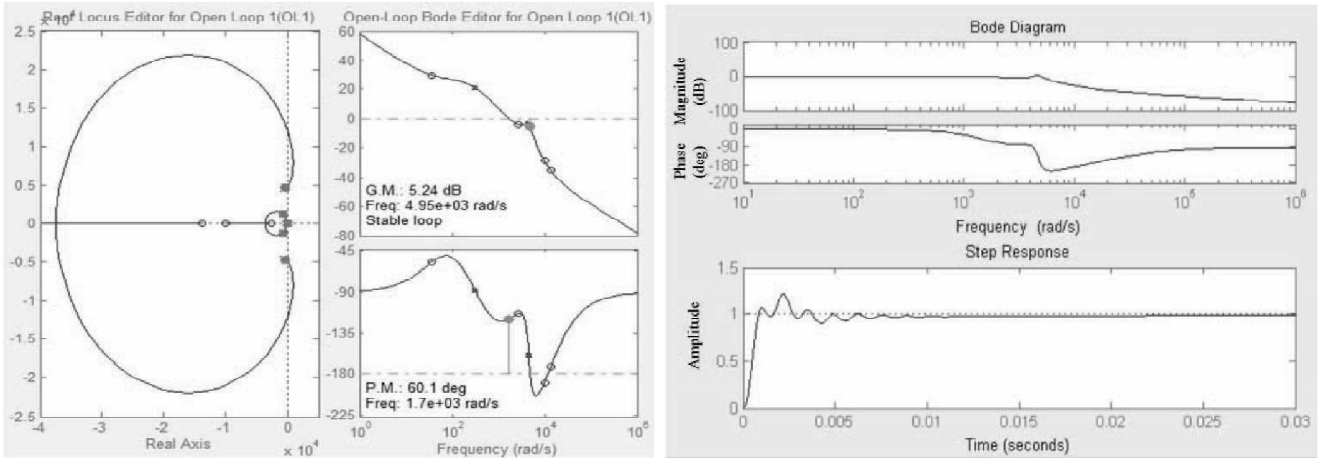

(a) (b)

Fig. 5.(a) Root locus and bode diagram of open loop system at K_p = 5.6, K_r= 6000, (b) Bode diagram of closed loop system and step response forK_p = 5.6, K_r= 6000.

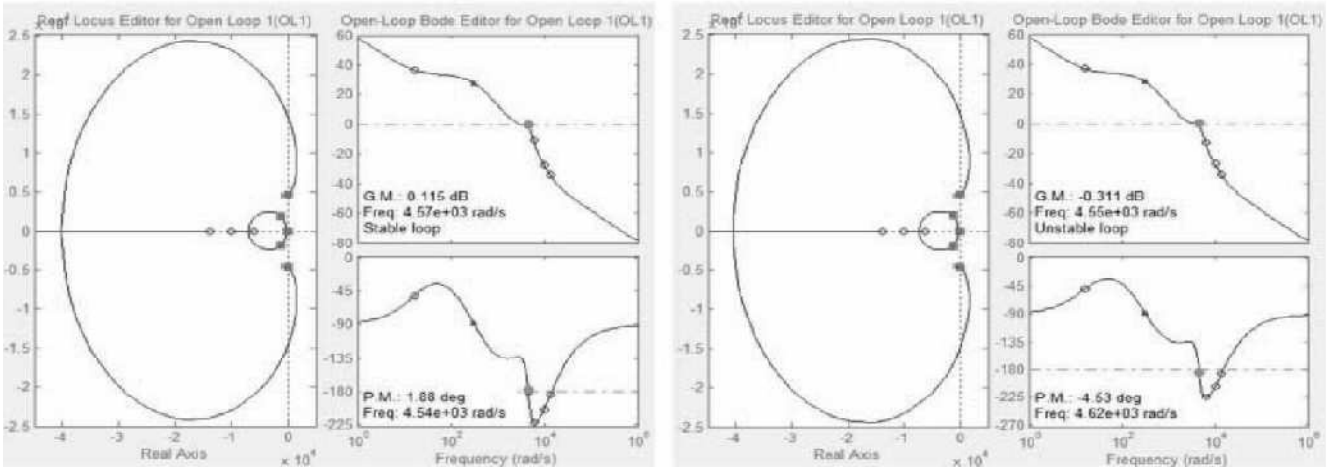

(a) (b)

Fig. 6. (a) Root Locus and Bode Diagram of Open Loop System for K_p =5.6, K_r=15000, (b) Root Locus and Bode Diagram of Open Loop System for K_p =5.6, K_r=16000

B. Simulation of Full Structure of the Proposed System

The proposed structure shown in Fig. 1, Fig. 3 and the system parameters listed in Table I have been considered in the simulation. The value of K_p is kept at 5.6 while K_r = 6000 and the results are shown in per unit values. The time step applied in the simulation is at t=0.1s. The proposed method works as it is required to, and is able to track the current reference as shown in Fig. 7(a). It shows how the VF estimation is significantly contributing to the effectiveness of the overall system with just a little overshoot on the current. Transients occurring in VF estimation during start up time are quickly attenuated and the system reaches its steady state after 0.05s which is at t=0.15s. The advantages of using the SOGI-QSG as well as proper tuning of K_p and K_r helps the system to have a faster tracking time where it can be seen that once the time step is applied, the PR current controller is able to force the converter output current to track the current reference almost immediately.

Fig. 7(b) and Fig. 7(c)shows the positive sequence current component of the converter side of the filter inductor and the output of the VF estimation respectively. The alpha and beta component of current and VF estimation have same amplitude with the beta component lagging the alpha by 90°. The output of VF estimation is very important because without correct estimation, the PR current controller will not be able to track the current reference as this output has been used in the reference current calculation. The active power reference, P_{ref} has been set to 10kW while the reactive power reference, Q_{ref} is set to zero. The measured active power and the reactive power of the system are matched with the active power reference and reactive power reference that have been set as shown in Fig. 7(d) and Fig. 7(e). One of the advantages of using the PR current controller is shown in Fig. 7(f) where the proposed system capable to achieve zero steady state error.

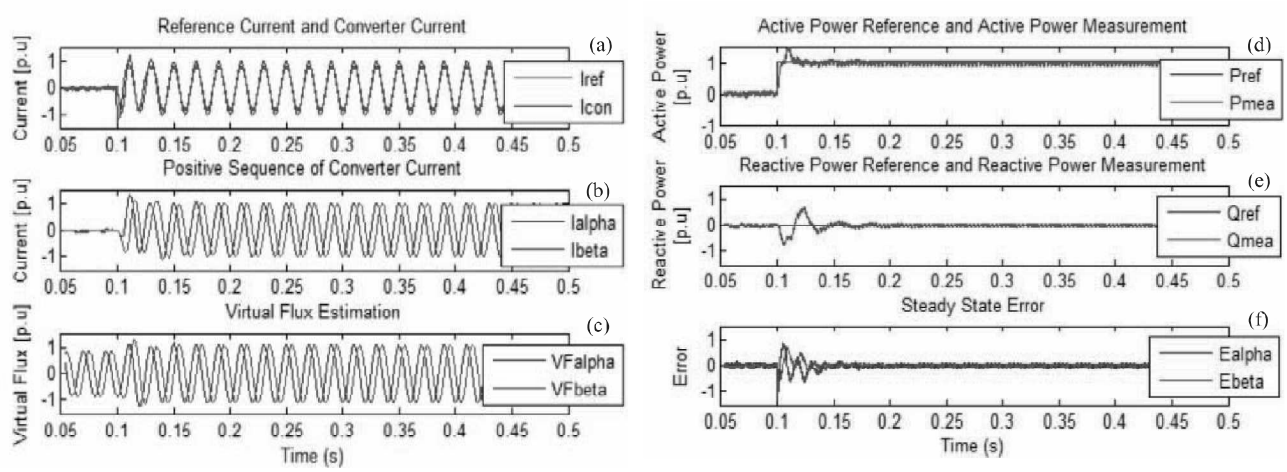

Fig. 7.Simulation results showing the operation of DSOGI-VF estimation with LCL Filter.

V. CONCLUSIONS

In this paper, the use of Proportional Resonant Current Controllers is proposed together with an implementation of VF estimation adapted for voltage sensor-less operation of grid connected VSCs with LCL filters. The relevance of this study is clearly supported by the stability analysis and the simulation results presented. For obtaining fully grid voltage sensor-less VF estimation with the LCL filter, the currents in the filter capacitors as well as the positive and negative sequence components of the grid currents must be estimated. The proposed implementation is taking advantage of the SOGI-QSG structure to ensure a simple and effective implementation with inherently frequency-adaptive characteristics. This study has shown that the VF estimation obtained is reliable and can be used in the current reference calculation for the inner current controller. The proposed VF estimation with the LCL filter has extended the dimension of previous work and most importantly has been demonstrated to work well with the inner current controller. With a proper tuning of the K_p and K_r as well as a proper characterization of the LCL filter, a good dynamic response can be achieved where the stability of the system is ensured.

ACKNOWLEDGEMENT

This work was supported in part by Spanish Ministry of Economy and Competitiveness under Project ENE2014-60228-R. Any opinions, findings, and conclusions or recommendations expressed in this material are those of the authors and do not necessarily reflect those of the host institutions or founders.

REFERENCES

[1] R. Teodorescu, M. Liserre, P. Rodriguez, 2011, "Grid Converters for Photovoltaic and Wind Power Systems," John Wiley & Son, United Kingdom

[2] Hansen, S., Malinowski, M., Blaabjerg, F., & Kazmierkowski, M. P., "Sensorless control strategies for PWM rectifier," in*Applied Power Electronics Conference and Exposition, (APEC 2000)*, vol. 2, pp. 832–838, 2000.

[3] Malinowski, M., Kazmierkowski, M. P., Hansen, S., Blaabjerg, F., & Marques, G. D., "Virtual-flux-based direct power control of three-phase PWM rectifiers," in*Industry Applications, IEEE Transactions 37*, pp. 1019–1027, 2001.

[4] Suul, J. A., & Undeland, T, "Impact of Virtual Flux reference frame orientation on voltage source inverters in weak grids," in*2010 International Power Electronics Conference - ECCE ASIA*, pp. 368–375, 2010.

[5] Suul, J. a., & Undeland, T., "Flexible reference frame orientation of Virtual Flux-based Dual Frame Current controllers for operation in weak grids," in*2011 IEEE Trondheim PowerTech*, pp. 1–8, 2011.

[6] Suul, J. A., Molinas, M. & Rodríguez, P., "Exploring the Range of Impedance Conditioning by Virtual Inductance for Grid Connected Voltage Source Converters", pp. 1–9, 2012.

[7] Malinowski, M., Marques, G., Cichowlas, M., & Kazmierkowski, M., "New direct power control of three-phase PWM boost rectifiers under distorted and imbalanced line voltage conditions," in*IEEE International Symposium on Industrial Electronics,*2003.

[8] Malinowski, M., Kazmierkowski, M. P., & Trzynadlowski, A. M., "A comparative study of control techniques for PWM rectifiers in AC adjustable speed drives," in*Power Electronics, IEEE Transactions*, *18*, pp. 1390–1396, 2003.

[9] Jasinski, M., Kazmierkowski, M. P., Bobrowska, M., & Okon, P., "Control of AC-DC-AC converter under unbalanced and distorted input conditions," in*CPE 2009 - 6th International Conference-Workshop - Compatability and Power Electronics*, pp. 139–145, 2009.

[10] Kulka, A., 2009, "Sensorless digital control of grid connected three phase converters for renewable sources," Ph.D Dissertation, Norwegian Univ. Sci. Technology, Trondheim, Norway

[11] Suul, J.A., 2012,"Control of Grid Integrated Voltage Source Converters Under Unbalanced Conditions – Development of an Online Frequency Adaptive Virtual Flux Based Approach," Ph.D Dissertation, Norwegian Univ. Sci. Technology, Trondheim, Norway.

[12] Suul, J. A., Luna, A., Rodriguez, P., & Undeland, T., "Frequency-adaptive Virtual Flux estimation for grid synchronization under unbalanced conditions," *IECON 2010 - 36th Annual Conference on IEEE Industrial Electronics Society*, vol. 1, pp. 486–492, 2010.

[13] Suul, J. A., Luna, A., Rodríguez, P., Member, S., & Undeland, T., "Voltage-Sensor-Less Synchronization to Unbalanced Grids by Frequency-Adaptive Virtual Flux Estimation," *IEEE Transactions on Industrial Electronics, 59*(7), pp. 2910–2923, 2012.

[14] Wrona, G, Malon, K, "Sensorless Operation of an Active Front End Converter with LCL filter," in 2014 IEEE 23rd International Symposium on Industrial Electronics, ISIE 2014, Istanbul, Turkey, pp. 2697-2702, 1-4 June 2014.

[15] Liserre, M., Blaabjerg, F., & Hansen, S., "Design and control of an LCL-filter-based three-phase active rectifier," in*IEEE Transactions on Industry Applications, 41*(5), pp. 1281–1291, 2005.

[16] Reznik, A, Simoes, M. G., Al-Durra, A, & Muyeen, S. M., "LCL filter design and performance analysis for small wind turbine systems," in*Power Electronics and Machines in Wind Applications (PEMWA-2012),* pp. 1-7, 2012.

[17] Zammit, D., Staines, C. S., & Apap, M., "Comparison between PI and PR Current Controllers in Grid Connected PV Inverters," in*International Journal of Eletrical, Computer, Electronics and Communication Engineering)*, 8(2), pp. 224-229, 2014.

[18] Teodorescu, R., Blaabjerg, F., Liserre, M., & Loh, P. C., "Proportional-resonant controllers and filters for grid-connected voltage-source converters," in*IEE Proceedings - Electric Power Applications*, *153*(5), pp. 750-762, 2006.